



## Node-free seven-tube hollow-core anti-resonant fiber for low-loss broadband optical transmission

Arpita Pradhan<sup>1</sup>, Ashutosh Pratap Singh<sup>2</sup>, Bishnu P Pal<sup>1</sup> and Somnath Ghosh<sup>1</sup>

<sup>1</sup>Department of Physics, École Centrale School of Engineering, Mahindra University, Hyderabad, Telangana, 500 043, India

<sup>2</sup>Department of Physics, Institute of Science, Banaras Hindu University, Varanasi-221 005, India

(In loving memory of Revered Professor M. S. Sodha)

We present a detailed investigation to understand the impact of the number of node-type and node-free circular cladding tubes in the context of hollow-core anti-resonant fibers (HC-ARFs) and propose an optimized design that enables low-loss transmission while supporting effective single-mode operation across the telecommunication wavelength band. For the node-free seven-tube HC-ARF design, the proposed structure achieves a total loss below 0.1 dB/km within the telecommunication wavelength range, covering the O-band to the U-band, and exhibits a peak higher-order mode extinction ratio (HOMER)  $\approx 3044$  at 1.55  $\mu\text{m}$ . We also evaluate the large effective mode area to be  $A_{\text{eff}} \approx 4227 \mu\text{m}^2$ . Furthermore, a fabrication tolerance analysis is incorporated to ascertain the robustness of the structure. This fiber holds strong potential for applications in future high-speed optical communication networks. © Anita Publications. All rights reserved.

doi: [10.54955/AJP.34.11-12.2025.677-683](https://doi.org/10.54955/AJP.34.11-12.2025.677-683)

**Keywords:** Hollow core anti-resonant fiber, low loss, large bandwidth.

### 1 Introduction

In recent years, hollow-core fibers (HCFs) have attracted significant attention for numerous applications owing to their unique structural design and guiding mechanisms for exceptional transmission characteristics compared to conventional solid-core fibers [1,2]. In these fibers, the central air core guides up to 99.9% of the optical power, with only a minimal fraction interacting with the surrounding glass tubes. This capability opens up a wide range of possibilities; for example, air-core guidance significantly enhances the optical damage threshold [3], making hollow-core anti-resonant fibers (HC-ARFs) highly suitable for high-power laser delivery [4,5]. The presence of an air core, which if filled with gases or fluids, enables applications in sensing [6,7] and studies in gas-based nonlinear optics [7,8]. In telecommunications, the potential increase in transmission speed offers significant advantages for applications in defense, finance, data-processing hubs, and any area where high-speed data transfer is essential.

HCFs are classified into two categories based on the light-guidance mechanism. The first category is the hollow-core photonic bandgap (HC-PBG) fiber, where light is guided within the air core via the photonic bandgap effect. These fibers have achieved a minimum loss of roughly 1.2 dB/km in the telecommunications band [9,10]. The other category of hollow-core fiber, commonly known as hollow-core anti-resonant fibers (HC-ARFs), involves light confinement arising from inhibited coupling with the modes of the surrounding glass tubes [11,12].

Corresponding author

e mail: [somiit@rediffmail.com](mailto:somiit@rediffmail.com) (Somnath Ghosh)

The HC-ARFs have attracted significant attention due to their exceptional transmission characteristics, including wide bandwidth, low loss, low dispersion, and minimal optical power confinement within the glass regions. An early realization of inhibited-coupling fibers was the Kagome fiber, first demonstrated by Benabid *et al* [13]. Unlike hollow-core photonic bandgap fibers (HC-PBG), AR-HCFs are characterized by a simpler single-ring cladding structure and a comparatively larger core-diameter-to-wavelength ratio. In HC-ARFs, the thin capillary wall surrounding the core acts as a Fabry-Perot resonator [14]. Hollow-core fibers with circular cladding tubes, such as double-nested hollow-core fibers (DNANF), have demonstrated ultra-low optical attenuation, with the lowest reported loss of  $< 0.11$  dB/km at  $1.55 \mu\text{m}$  [15], offering better performance than HC-PBG fibers. This shows strong potential to eventually exceed the Rayleigh scattering limit of standard silica optical fibers [16].

In this work, we have examined the propagation loss of the fundamental mode (FM) across different HC-ARF structures to investigate the impact of cladding parameters. Our numerical investigation reveals that the number of cladding anti-resonant tubes plays a decisive role in minimizing propagation loss and broadening the transmission bandwidth. Through this study, we identify an optimized design that maintains low confinement loss while ensuring robust single-mode guidance. Specifically, we analyze hollow-core anti-resonant fibers (HC-ARFs) with six, seven, and nine cladding tubes, where the nine-tube configuration exhibits the lowest theoretical loss. However, to ensure fabrication feasibility and structural reliability, we propose a node-free seven-tube HC-ARF. For this geometry, we conduct a comprehensive performance analysis encompassing single-mode guidance characteristics, spectral transmission behaviour, effective mode area, and fabrication tolerance under different structural variations.

## 2 Fiber Design

To investigate low-loss light guidance, we conduct numerical simulations of three hollow-core anti-resonant fiber (HC-ARF) designs with six, seven, and nine cladding tubes. The schematic representations of these structures, depicted in Fig 1, form the basis of the numerical simulations conducted in this work.

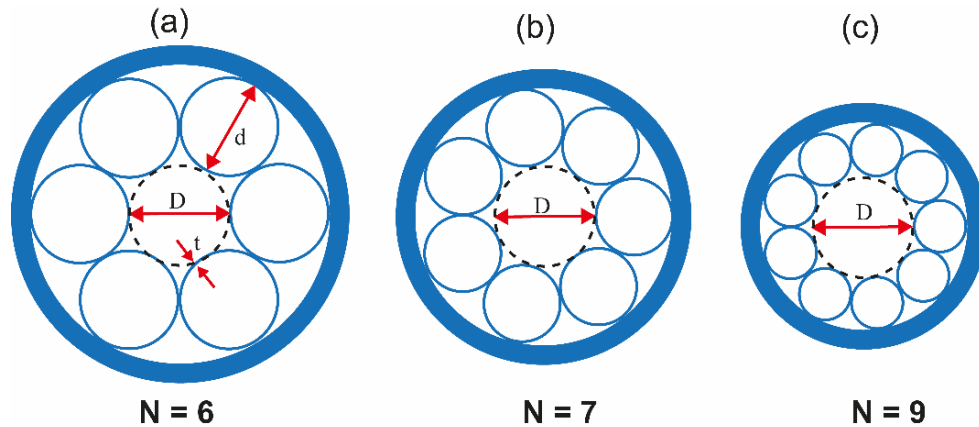


Fig 1. Schematic diagram of HC-ARF with (a) six-, (b) seven-, and (c) nine-cladding tubes.

In this work, the hollow-core anti-resonant fiber (HC-ARF) core diameter ( $D$ ) is taken as  $100 \mu\text{m}$ , and the gap between two adjacent cladding tubes ( $g$ ) is assumed to be zero for all the studied structures. The cladding tube diameter ( $d$ ) is calculated using the following relation for different values of  $N$ .

$$d = \frac{g - D \cdot \sin(\pi/N)}{\sin(\pi/N) - 1}$$

Here,  $N$  represents the number of cladding tubes [16]. The value of the diameter of the cladding tubes ( $d$ ), expressed in  $\mu\text{m}$ , for  $N = 6, 7$ , and  $9$  are calculated to be  $100 \mu\text{m}$ ,  $76.64 \mu\text{m}$ , and  $51.98 \mu\text{m}$ , respectively. To achieve anti-resonant guidance at  $1.55 \mu\text{m}$ , the cladding tube thickness is appropriately selected. The anti-resonant tube thickness ( $t_{AR}$ ) is found to be  $0.37 \mu\text{m}$ , obtained using the relation reported in [7].

$$t_{AR} = \frac{1}{4} \frac{\lambda}{\sqrt{n_g^2 - 1}}$$

where  $n_g$  is the refractive index of the glass of cladding tubes at  $\lambda = 1.55 \mu\text{m}$ .

### 3 Propagation Characteristics

We simulated the fibers using the Ansys Lumerical™ software. Figure 2(a) shows the mode field profile of the fundamental mode like  $LP_{01}$  of the nine-tube HC-ARF. The mode appears to be well confined in the air core, with negligible power in the cladding. The loss values were obtained by using material data for pure silica and included confinement and absorption losses. In our current calculations, we have ignored the surface scattering loss.

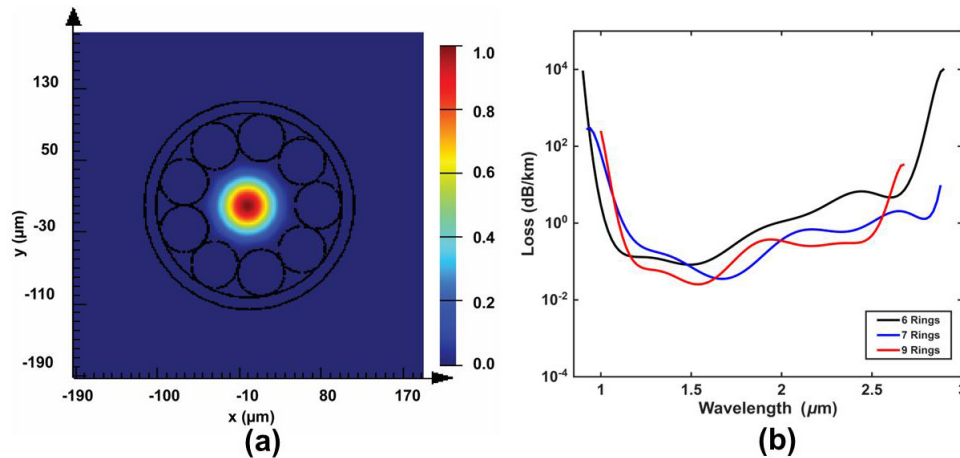


Fig 2. (a) Mode field profile of a nine-tube node-type HC-ARF design. (b) Computed loss spectra of the six-, seven-, and nine-tube node-type HC-ARF design.

Here, we analyze the impact of varying the number of anti-resonant cladding tubes on the propagation loss. Initially, we make a direct comparison between regular HC-ARFs with six, seven, and nine cladding tubes. The results clearly indicate that the nine-tube HC-ARF exhibits superior loss performance, with lower attenuation and a broader transmission window, compared to the six and seven-tube fibers. As shown in Fig 2(b), for the nine-tube structure, the total loss is approximately  $0.1 \text{ dB/km}$  over the  $1.4\text{--}1.6 \mu\text{m}$  wavelength range, with the loss being around  $0.02 \text{ dB/km}$  around  $1.55 \mu\text{m}$  wavelength. This is much lower compared to the theoretical low-loss limit of  $0.14 \text{ dB/km}$  of conventional solid-core silica fibers. The wider transmission window and reduced loss of this fiber can be attributed to the smaller distance between the surrounding outer tube and the core compared to the six and seven-tube fibers. The mode effective area of the fundamental mode of the fiber is  $\sim 4100 \mu\text{m}^2$  at  $1.55 \mu\text{m}$  wavelength.

In this work, we explored a node-free, seven-tube HC-ARF design, depicted in Fig 3(a). For effective suppression of higher-order modes (HOM) and to achieve fundamental mode guidance, the optimal cladding-to-core diameter ratio is found to be  $d/D = 0.68$  [12]. In contrast to the previously investigated nine-tube node-type structure, which showed slightly lower simulated confinement loss, the node-free design offers significant fabrication advantages. These include reduced structural complexity and improved tolerance to

geometric imperfections during preform assembly. As shown in Fig 3(b), the simulated loss spectrum of the fundamental mode like  $LP_{01}$  reveals a total loss below 0.1 dB/km across a wide wavelength range from 1.2  $\mu\text{m}$  to 2.1  $\mu\text{m}$ , making the design promising for low-loss transmission.

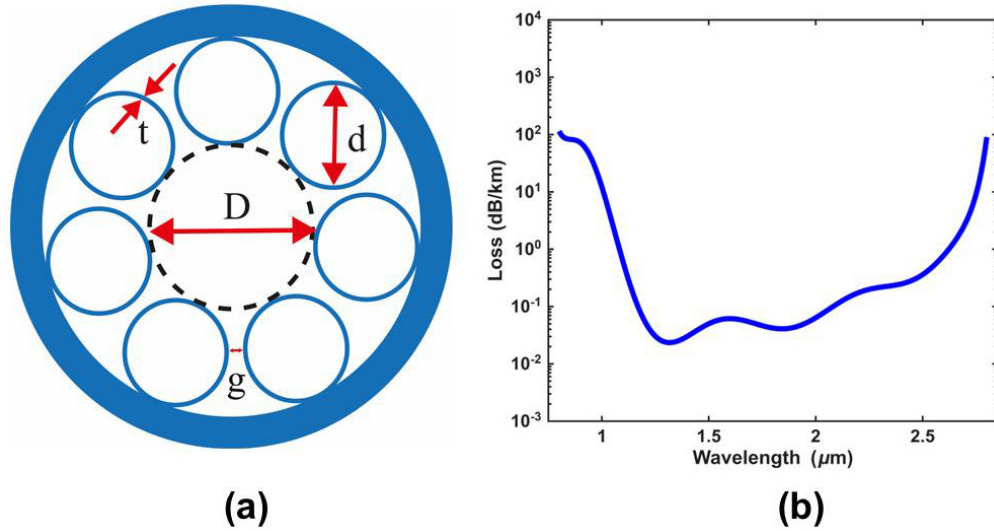


Fig 3. (a) Schematic of a node-free seven-tube HC-ARF. (b) Computed loss spectrum of the fundamental  $LP_{01}$  mode for the node-free seven-tube HC-ARF.

Figure 4(a) presents the calculated differential loss between the  $LP_{01}$  and  $LP_{11}$  modes, revealing an average suppression of 150 dB/km across 1.50–1.60  $\mu\text{m}$ . This high intermodal loss difference ensures robust single-mode guidance, with the design achieving a peak higher-order mode extinction ratio (HOMER) of approximately 3044 at 1.55  $\mu\text{m}$ .

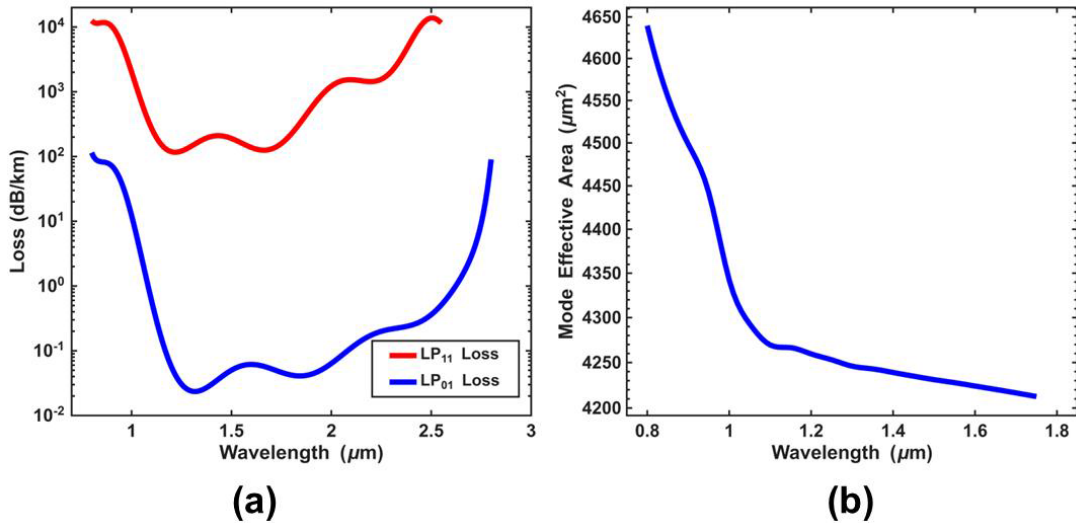


Fig 4. (a) The computed loss spectra of node-free seven tube HC-ARF with differential loss of around 150 dB/km between  $LP_{01}$  and  $LP_{11}$  in the telecommunication band over 1.5  $\mu\text{m}$  to 1.6  $\mu\text{m}$ . (b) Variation of mode effective area ( $A_{eff}$ ) as a function of wavelength.

Furthermore, Fig 4(b) illustrates the wavelength dependence of the mode effective area ( $A_{eff}$ ), which attains  $4227 \mu\text{m}^2$  at  $1.55 \mu\text{m}$ . This value slightly exceeds that of the nine-tube node-type HC-ARF design ( $A_{eff} \approx 4100 \mu\text{m}^2$ ), indicating that the present seven-tube node-free configuration offers greater spatial mode expansion. The increase in  $A_{eff}$  contributes to the suppression of nonlinear optical effects, including self-phase modulation and stimulated Brillouin scattering, thereby making the structure more favourable for high power optical signal delivery. This improvement, combined with its fabrication-friendly geometry, strengthens the potential of the node-free design for high-capacity communication and power transmission applications.

#### 4 Tolerance Study

In this study, a comprehensive tolerance analysis was performed to assess the impact of potential fabrication imperfections on the performance of the proposed fiber structures, with particular focus on variations in cladding thickness and diameter.

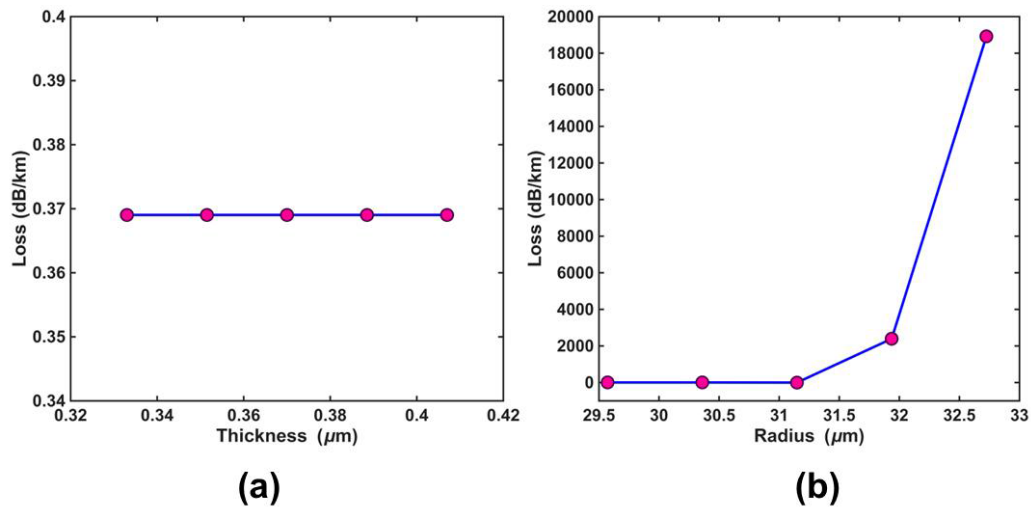


Fig 5. (a) Impact of  $\pm 5\%$  variation in cladding tube thickness, and (b) variation in the cladding tube radius, where the loss remains nearly unchanged (with only a slight increase from  $< 0.1$  dB/km) for deviations within  $\pm 2\%$ .

As shown in Fig 5(a), the proposed HC-ARF design exhibits exceptional resilience to fabrication errors, maintaining nearly constant loss for thickness variations up to  $\pm 5\%$ . These results clearly indicate that the fiber sustains stable performance under such dimensional variations, thereby highlighting its strong fabrication tolerance.

In contrast, Fig 5(b), the HC-ARF with a node-free seven-tube cladding configuration exhibits total loss that remains largely unaffected for minor dimensional variations of up to  $\pm 2\%$ , whereas deviations beyond this threshold result in a pronounced increase in loss.

#### 5 Conclusion

It is observed that, for a nine-tube HC-ARF, the propagation loss can be reduced to below  $0.03$  dB/km at  $1.55 \mu\text{m}$ , while remaining below  $0.1$  dB/km over a wide wavelength range from  $1.2 \mu\text{m}$  to  $1.72 \mu\text{m}$ . This effectively opens up a larger bandwidth with an average loss value smaller than the already reported values, and is far below the theoretical loss limit of conventional solid-core silica fibers in this region [17]. In conclusion, we have identified design parameters for an HC-ARF that achieves propagation losses of

less than 0.1 dB/km in the telecommunication wavelength window, with a large mode area of  $4100 \mu\text{m}^2$  at  $1.55 \mu\text{m}$ . To ensure fabrication feasibility, we investigated another HC-ARF with node-free seven-tube, which exhibits a propagation loss of 0.06 dB/km at  $1.55 \mu\text{m}$ , while maintaining the loss below 0.1 dB/km over a wide wavelength range from  $1.17 \mu\text{m}$  to  $2.1 \mu\text{m}$ . The design also offers a large effective mode area of  $A_{\text{eff}} = 4227 \mu\text{m}^2$ , which is higher than that of the nine-tube HC-ARF ( $A_{\text{eff}} = 4100 \mu\text{m}^2$ ). This could open up possibilities for high-speed DWDM signal transmission through these fibers in the telecommunication wavelength window.

### Acknowledgement

The authors acknowledge the financial support in the form of an assistantship for pursuing of Ph D, from Mahindra University, Hyderabad, India.

### Data availability

The data will be made available on request.

### Disclosure

The authors declare no conflict of interest.

### References

1. Ding W, Wang Y.-Y, Gao S.-F, Wang M.-L, Wang P, Recent Progress in Low-Loss Hollow-Core Anti-Resonant Fibers and Their Applications, *IEEE J Sel Top Quantum Electron*, 26(2020)1–12.
2. Fokoua E N, Mousavi S A, Jasion G T, Richardson D J, Poletti F, Loss in hollow-core optical fibers: mechanisms, scaling rules, and limits, *Adv Opt Photonics*, 15(2023)1–85.
3. Sakr H, Chen Y, Jasion G T, Bradley T D, Hayes J R, Mulvad H C H, I. Davidson I A, Fokoua E N, Poletti F, Hollow core optical fibres with comparable attenuation to silica fibres between 600 and 1100 nm, *Nat Commun* 11(2020)6030; doi.org/10.1038/s41467-020-19910-7.
4. Lee S.-Y, Current optics and photonics, *Curr Opt Photonics*, 1(2017)239–246.
5. Yan S, Lou S, Wang X, Zhang W, Zhao T, Single-mode large-mode-area double-ring hollow-core anti-resonant fiber for high power delivery in mid-infrared region, *Opt Fiber Technol*, 46(2018)118–124.
6. Belardi W, SSDesign and Properties of Hollow Antiresonant Fibers for the Visible and Near Infrared Spectral Range, *J Light Technol*, 33(2015)4497–4503.
7. Travers J C, Chang W, Nold J, Joly N Y, Russell P S J, Ultrafast nonlinear optics in gas-filled hollow-core photonic crystal fibers [Invited], *J Opt Soc Am B*, 28(2011)A11-A26.
8. Russell P S J, Hölzer P, Chang W, Abdolvand A, Travers J C, Hollow-core photonic crystal fibres for gas-based nonlinear optics, *Nat Photonics*, 8(2014)278–286.
9. Poletti F, Petrovich M N, Richardson D J, Li M J, Hollow-core photonic bandgap fibers: Technology and applications, *Nanophotonics*, 2(2013)315–340.
10. Bradley T D, Hayes J R, Chen Y, Jasion G T, Sandoghchi S R, Slavik R, Fokoua E N, Bawn S, Sakr H, I.A. Davidson I A, Taranta A, Thomas J P, Petrovich M N, Richardson D J, Poletti F, Record Low-Loss 1.3 dB/km Data Transmitting Antiresonant Hollow Core Fibre, 2018 European Conference on Optical Communication (ECOC), 2018, pp 1–3.
11. Poletti F, Nested antiresonant nodeless hollow core fiber, *Opt Express*, 22(2014)23807– 23828.
12. Habib M S, Bang O, Bache M, Low-loss single-mode hollow-core fiber with anisotropic anti-resonant elements, *Opt Express*, 24(2016)8429–8436.
13. Benabid F, Knight J C, Antonopoulos G, Russell P S J, Stimulated Raman Scattering in Hydrogen-Filled Hollow-Core Photonic Crystal Fiber, *Science*, 298(2002) 399–402.

14. Litchinitser N M, Abeeluck A K, Headley C, Eggleton B J, Antiresonant reflecting photonic crystal optical waveguides, *Opt Lett*, 27(2002)1592–1594.
15. Chen Y, Petrovich M N, Fokoua E N, Adamu A I, Hassan M R A, Sakr H, Slavik R, Gorajooobi S B, Alonso M, Ando R F, Papadimopoulos A, Varghese T, Wu D, Ando M F, Wisniowski K, Sandoghchi S R, Jasion G T, Richardson D J, Poletti F, Hollow Core DNANF Optical Fiber with  $< 0.11$  dB/km Loss, in Optical Fiber Communication Conference (OFC), 2024, (Optica Publishing Group, 2024), p. Th4A.8.
16. Gao S, Wang Y, Ding W, Hong Y, Wang P, Conquering the Rayleigh Scattering Limit of Silica Glass Fiber at Visible Wavelengths with a Hollow-Core Fiber Approach, *Laser Photon Rev*, 14(2020); doi.org/10.1002/lpor.201900241.
17. Petrovich M, Numkam Fokoua E, Chen Y, Sakr H, Adamu A I, Hassan R, Wu D, Fatobene Ando R, Papadimopoulos A, Sandoghchi S R, Jasion G, Poletti F, Broadband optical fibre with an attenuation lower than 0.1 decibel per kilometre, *Nat Photonics*, 19(2025)1203–1208.

[Received: 26.08.2025; revised recd: 26.12.2025; accepted: 29.12.2025]